### The Geodesic Equations in a Two-Dimensional Finsler Manifold Equipped with a Matsumoto-Type Metric-II

B. K. Tripathi, V. K. Chaubey and S. Prajapati

**Abstract.** This paper provides a comprehensive derivation of geodesic equations in a two-dimensional Finsler space characterized by a Matsumoto-type metric. It further explores the geometric applications of these equations on various surfaces, including cylinders, spheres, pseudo-spheres, and catenoids. Using illustrative examples and graphs, we analyze the geometric properties of geodesics for different parametric forms of these surfaces. The results enhance our understanding of geodesic behavior in Finsler geometry and shed light on curvature and geometric structures in diverse contexts.

Key Words: Finsler Space,  $(\alpha, \beta)$ -Metric, Matsumoto-Type  $(\alpha, \beta)$ -Metric, Geodesic

Mathematics Subject Classification 2020: 53B40, 53C60

#### Introduction

In 1972, Matsumoto introduced a special Finsler metric by considering the positively homogeneous function  $L(\alpha, \beta)$  of degree one in  $\alpha$ , represented by  $\sqrt{a_{ij}(x)y^iy^j}$ , which corresponds to a Riemannian metric, and  $\beta(x,y)$  expressed as  $b_i(x)y^i$  serves as a one-form metric [5–7].

Let us consider a special form of the class p-power  $(\alpha, \beta)$ -metric, as studied in [13–15]. Its generalized expression is given by

$$L(\alpha, \beta) = \alpha^{1-p} (\alpha + \beta)^p,$$

where  $p \in \mathbb{R} \setminus 0$ . Notably, when p = -m, this metric transforms into the following form:

$$L(\alpha, \beta) = \alpha^{m+1} (\alpha + \beta)^{-m}. \tag{1}$$

This form aligns with the Matsumoto-type metric. An intriguing feature of this metric is its convergence to the Riemannian metric when  $\alpha$  exceeds  $\beta$ , as the ratio  $\alpha(\alpha + \beta)^{-1}$  tends to 1 in such cases.

Geodesics play a vital role in defining the shortest paths between points and are fundamental for grasping space geometry. Matsumoto and Park [8] first explored this concept in 1997, specifically investigating Randers and Kropina metrics. Additionally, Matsumoto collaborated with H. S. Park in [9] to extend this concept to the Matsumoto metric, which is used to measure the slope of a mountain. Subsequently, various authors (see, for example, [2–4, 10–12]) have examined the differential equations governing geodesics in two-dimensional scenarios, and their studies have deepened our understanding of geometric properties within Finsler spaces by exploring various forms of Finsler metrics.

In this paper, we find out the geodesic equations within a two-dimensional Finsler space equipped with Matsumoto-type metric defined by equation (1) and explores its geometric applications on various surfaces like cylinders, spheres, pseudo-spheres, and catenoids. Through diverse illustrative examples and graphs, we find out the geometric properties of geodesics for various parametric forms of cylinders, spheres, and catenoids.

#### 1 Preliminaries

Matsumoto and Park [8,9] wrote out the differential equation of the geodesic problem in a Finsler space  $F^2 = (M^2, L(\alpha, \beta))$  equipped with the  $(\alpha, \beta)$ -metric, where the Finsler function L(x, y) relies on both the Riemannian metric  $\alpha$  and the 1-form  $\beta$ , under the following conditions:

(1) The two-dimensional manifold  $M^2$  is conceptualized as a surface S that can be described within a three-dimensional orthonormal coordinate system  $X^{\alpha}$ ,  $\alpha = 1, 2, 3$ . The parametric representation of S is given by  $X^{\alpha} = X^{\alpha}(x^1, x^2)$ . As S possesses an induced Riemannian metric, we introduce two tangent vector fields  $B_i$ , i = 1, 2, whose components are defined as  $B_i^{\alpha} = \partial X^{\alpha}/\partial x^i$ , and the components of the metric tensor are  $a_{ij} = \sum_{\alpha} B_i^{\alpha} B_j^{\alpha}$ .

Considering the isothermal coordinate system  $x^i = (x^1, x^2) = (x, y)$  on the surface S, the Riemannian metric is denoted as  $\alpha = aE$ , where a = a(x, y) > 0 and E represent the Euclidean distance function given by  $E = \sqrt{\dot{x}^2 + \dot{y}^2}$ . The computation of Christoffel coefficients for S is accomplished using the following formula:

$$\Gamma_{ij}^{h} = \frac{a^{kh}}{2} \left\{ \frac{\partial a_{jk}}{\partial x^{i}} + \frac{\partial a_{ik}}{\partial x^{j}} - \frac{\partial a_{ij}}{\partial x^{k}} \right\}.$$

Subsequently, in the isothermal co-ordinate system  $(x^1, x^2) = (x, y)$ , the Christoffel coefficients  $\Gamma_{ij}^h(x, y)$  are determined as

$$\left(\Gamma_{11}^1,\Gamma_{12}^1,\Gamma_{22}^1;\Gamma_{11}^2,\Gamma_{12}^2,\Gamma_{22}^2\right) = \left(\frac{a_x}{a},\frac{a_y}{a},-\frac{a_x}{a},-\frac{a_y}{a},\frac{a_x}{a},\frac{a_y}{a}\right).$$

Note that in this paper, we use the symbol (;) to signify covariant differentiation concerning Christoffel symbols within  $\mathbb{R}^2$ .

(2) Let  $B = B^{\alpha}$  be a constant vector field within the ambient 3-space. Along the surface S, this constant vector field B can be expressed as

$$B = b^i B_i + b^0 N, (2)$$

where  $\beta = b_1 \dot{x} + b_2 \dot{y}$ , and  $b_i = a_{ij} b^j$  denotes the tangential component of B. Then the Gauss-Weingarten derivation formulae can then be formulated as

$$B_{;j} = (b_{;j}^i B_i + b^i H_{ij} N) + (b_{;j}^0 N - b^0 H_j^i B_i),$$

where  $H_{ij} = a_{ik}H_j^k$  represents the second fundamental tensor of surface S. If  $B_{;j} = 0$ , we obtain  $b_{;j}^i = b^0H_j^i$ , leading to

$$b_{i;j} = b^0 H_{ij}. (3)$$

This result further leads to  $b_{i;j} = b_{j;i}$ , specifically,  $b_{1y} = b_{2x}$ , indicating that  $b_i$  is a gradient vector field within S.

(3) In the context of the Finslerian surface S, the linear form  $\beta$  originates from Earth's gravitational influence, as described in [8]. Consequently, we assume that the constant vector field B aligns with the  $X^3$ -axis, i.e.,  $B^a = (0,0,G)$  is a positive constant. This assumption leads to the expression  $G^2 = a_{ij}b^ib^j + (b^0)^2$  derived from equation (2). Given that  $(a_{11}, a_{12}, a_{22}) = (a^2, 0, a^2)$ , we can further deduce that

$$\left(\frac{G}{a}\right)^2 = (b^1)^2 + (b^2)^2 + \left(\frac{b^0}{a}\right)^2.$$

We focus on quantities of degree one by considering G/a as an infinitesimal of degree one and neglecting terms of degree two or higher. Thus,  $b^1, b^2$ , and  $b^0/a$  are considered to be of degree one. Equation (3) indicates that  $\beta_{;0}/a = (b_{i;j}\dot{x}^i\dot{x}^j)/a$  is also an infinitesimal of degree one. We denote these three infinitesimals of degree one as:

$$\mu = \frac{\gamma}{a^2}, \quad \nu = \frac{\beta_{;0}}{a}, \quad \lambda = \frac{\beta}{a^2},$$
 (4)

where  $\gamma = b_1 \dot{y} - b_2 \dot{x}$ .

The  $(\alpha, \beta)$ -metric F is characterized as a homogeneous function of degree one in both  $\alpha$  and  $\beta$ , as stated in [1]. Under the conditions

$$F_{\alpha\alpha}\alpha + F_{\alpha\beta}\beta = 0,$$
  
$$F_{\beta\alpha}\alpha + F_{\beta\beta}\beta = 0,$$

we derive the expression for  $\omega$ :

$$\omega = \frac{F_{\alpha\alpha}}{\beta^2} = -\frac{F_{\alpha\beta}}{\alpha\beta} = \frac{F_{\beta\beta}}{\alpha^2},$$

which is commonly referred to as the  $\omega$ -Weierstrass invariant for  $F(\alpha, \beta)$ .

Further, Matsumoto and Park [8] derived the differential equations for an  $(\alpha, \beta)$ -metric in a two-dimensional Finsler space with an isothermal coordinate system  $(x^1, x^2) = (x, y)$  as follows:

$$(L_{\alpha} + aE\omega\gamma^{2})F_{i}(c) - \beta_{;0}a^{2}\omega\gamma - L_{\beta}(b_{1y} - b_{2x}) = 0,$$
 (5)

where  $\omega$  represents the Weierstrass invariant, and  $F_i(c)$  is defined as:

$$F_i(c) = \frac{a(\dot{x}\ddot{y} - \dot{y}\ddot{x})}{E^3} + \frac{(a_x\dot{y} - a_y\dot{x})}{E}, i = 1, 2.$$

The equation  $F_i(c) = 0$  describes the geodesics in a given space, typically in the context of differential geometry. Here,  $F_i$  represents a set of equations related to the geometry, often involving the metric or curvature of the manifold in the associated Riemannian space, and the parameter C denotes a curve or path within that space.

# 2 Geodesics in Matsumoto-type $(\alpha, \beta)$ -metric space with $L = \alpha^{m+1}(\alpha + \beta)^{-m}$

The Finsler metric described by equation (1) is commonly known as a Matsumoto-type metric. To analyze this metric, we begin by considering an isothermal coordinate system  $(x^1, x^2) = (x, y)$  on the two-dimensional manifold  $(M^2, L)$ . Using equation (1) and the concept of partial derivatives, we can investigate the properties of the Matsumoto-type metric. Specifically, we can compute the derivatives of the metric components to explore their implications for curvature and geodesics, which are outlined below:

$$L_{\alpha} = \frac{\alpha^{m} \left\{ \alpha + (m+1)\beta \right\}}{(\alpha+\beta)^{m+1}}, \ L_{\beta} = -\frac{m\alpha^{m+1}}{(\alpha+\beta)^{m+1}}, \ \omega = \frac{m(m+1)\alpha^{m-1}}{(\alpha+\beta)^{m+2}}.$$
 (6)

Based on equations (4), (5) and (6), we derive the following result:

$$\left(1 + \frac{(m+2)a\lambda}{E} + \frac{(m+1)a^2}{E^2} \left(\lambda^2 + m\mu^2\right)\right) F_i(c) = \frac{m(m+1)a^2\nu\mu}{E^3}.$$

This equation establishes the relationship between the parameters  $a, \lambda, \mu, v, E$ , and the function  $F_i(c)$  derived from the initial set of equations. Next, by neglecting higher-order infinitesimals, we have:

$$F_i(c) = \frac{m(m+1)a^2v\mu}{E^3}. (7)$$

If x from (x, y) is the parameter t, we have  $(\dot{x}, \dot{y}) = (1, y')$  and  $(\ddot{x}, \ddot{y}) = (0, y'')$  with  $E = \sqrt{1 + y'^2}$  [12]. Therefore, we get

$$F_i(c) = \frac{ay''}{E^3} + \frac{(a_x y' - a_y)}{E}.$$
 (8)

By equating (7) and (8), we obtain the approximate geodesic equation for  $L = \alpha^{m+1}(\alpha + \beta)^{-m}$ :

$$y'' = \frac{m(m+1)\gamma\beta_{;0}^*}{a^2} - \frac{E^2}{a}(a_xy' - a_y), \tag{9}$$

where y' = dy/dx,  $a = |a_{ij}(x)|$ ,  $\gamma = b_1y' - b_2$  and

$$\beta_{;0}^* = b_{1;1} + (b_{1;2} + b_{2;1})y' + b_{2;2}(y')^2$$

$$= b_{1x} + (b_{1y} + b_{2x})y' + b_{2y}(y')^2$$

$$+ \frac{1}{a}(a_xb_1 + a_yb_2)(E^*)^2 - \frac{2}{a}(a_x + a_yy')(b_1 + b_2y').$$

Note that  $b_{1;2} = b_{2;1}$  and  $b_{1y} = b_{2x}$ .

Hence, we obtain the following result.

**Theorem 1** In a two-dimensional Finsler space employing an isothermal coordinate system  $(x^i)$ , the second-order differential equation (9) provides an approximation for the geodesics corresponding to the Matsumoto-type metric  $L = \alpha^{m+1}(\alpha + \beta)^{-m}$ .

# 3 Some examples in two-dimensional space employing geodesic

In this section, we shall use the following notation for geometric analysis:

$$(X^a) = (X, Y, Z), \quad (X^i) = (x, y).$$

Here,  $X^a$  represents coordinates in a three-dimensional space, while  $X^i$  represents coordinates in a two-dimensional plane.

### 3.1 Analyzing geodesic equations on a circular cylinder surface

**Example 1** Cylinder with X = ry. We examine a circular cylinder S:  $Y^2 + Z^2 = r^2$  and X = ry, which can be parametrically expressed as

$$S: X = ry, \quad Y = r\sin x, \quad Z = r\cos x.$$

From this parametrization, we derive the following basis vectors,  $B_1$ ,  $B_2$ , and the normal vector N:

$$B_{1} = \frac{\partial}{\partial x}(X, Y, Z) = (0, r \cos x, -r \sin x), \quad B_{2} = \frac{\partial}{\partial y}(X, Y, Z) = (r, 0, 0),$$
$$N = \frac{B_{1} \times B_{2}}{|B_{1} \times B_{2}|} = (0, -\sin x, -\cos x).$$

Since the metric coefficients are  $(a_{11}, a_{12}, a_{22}) = (r^2, 0, r^2)$ , we conclude that  $a_x = a_y = 0$ . Also, from (2), we have connection coefficients  $(b^1, b^2, b^0) = ((-G \sin x)/r, 0, -G \cos x)$  and  $(b_1, b_2) = (-Gr \sin x, 0)$ . Then

$$\beta_{0} = -Gr\cos x$$
 and  $\gamma = -Gr\sin xy'$ .

Consequently, we have the induced metric and  $\beta$ -term:

$$\alpha^2 = r^2 (dx^2 + dy^2), \quad \beta = -Gr \sin x \, dx.$$

Therefore, (9) gives the approximate differential equation of geodesic for a Matsumoto-type  $(\alpha, \beta)$ -metric (1) under the conditions of the above example in the form

$$y'' - \frac{m(m+1)}{2}G^2(\sin 2x) \ y' = 0,$$

which has a solution

$$y = c_1 \int_1^x e^{-\frac{1}{4}G^2 m(1+m)\cos 2x} dx + c_2.$$
 (10)

**Example 2** Cylinder with Y = ry. Consider the circular cylinder described by  $S: X^2 + Z^2 = r^2$  and Y = ry with parametric representation

$$S: X = r \cos x, \quad Y = ry, \quad Z = r \sin x.$$

From this parametrization, we derive the following basis vectors,  $B_1$ ,  $B_2$ , and the normal vector N:

$$B_1 = (-r\sin x, 0, r\cos x), \quad B_2 = (0, r, 0), \quad N = (-\cos x, 0, -\sin x).$$

The corresponding metric coefficients  $a_{ij}$  and the connection coefficients  $b^i$  and  $b_i$  are

$$(a_{11}, a_{12}, a_{22}) = (r^2, 0, r^2),$$
  $(b^1, b^2, b^0) = \left(\frac{G}{r}\cos x, 0, -G\sin x\right),$   $(b_1, b_2) = (Gr\cos x, 0).$ 

Additionally, we have  $a_x = a_y = 0$ . Then

$$\beta_{;0} = -Gr\sin x$$
 and  $\gamma = Gr\cos xy'$ .

Consequently, the following expressions for  $\alpha^2$  and  $\beta$ -term are obtained from the induced metric:

$$\alpha^2 = r^2 (dx^2 + dy^2), \quad \beta = Gr \cos x dx.$$

Thus, equation (9) provides the approximate differential equation of geodesic of a Matsumoto-type  $(\alpha, \beta)$ -metric (1) under the conditions of this example:

$$y'' + \frac{m(m+1)}{2}G^2(\sin 2x) \ y' = 0,$$

which has the solution

$$y = c_1 \int_1^x e^{\frac{1}{4}G^2 m(1+m)\cos 2x} dx + c_2.$$
 (11)

Thus, from Examples 1 and 2, we have

**Proposition 1** The differential equations for geodesics of the Matsumototype metric in a two-dimensional Finsler manifold, as examined in Examples 1 and 2 for a circular cylinder, are expressed as follows:

$$y'' \mp \frac{m(m+1)}{2}G^2(\sin 2x) \ y' = 0,$$

and their solutions, respectively, are expressed as

$$y = c_1 \int_1^x e^{\mp \frac{1}{4}G^2 m(1+m)\cos 2x} dx + c_2.$$

Since the solution derived in the above proposition cannot be obtained analytically, we resort to numerical methods using Python. For this purpose, we set G = 1 and  $c_2 = 0$ , as it serves merely as a shifting parameter. We then explore the behavior of the solution for various values of  $c_1 = 1, 2, 3$  and m = 1, 2, 3. The results corresponding to these parameter variations are presented in Figure 1.

In Figure 1, the first graph illustrates the behavior of the function given in equation (10) for different values of  $c_1$  and m. Since the integrand is

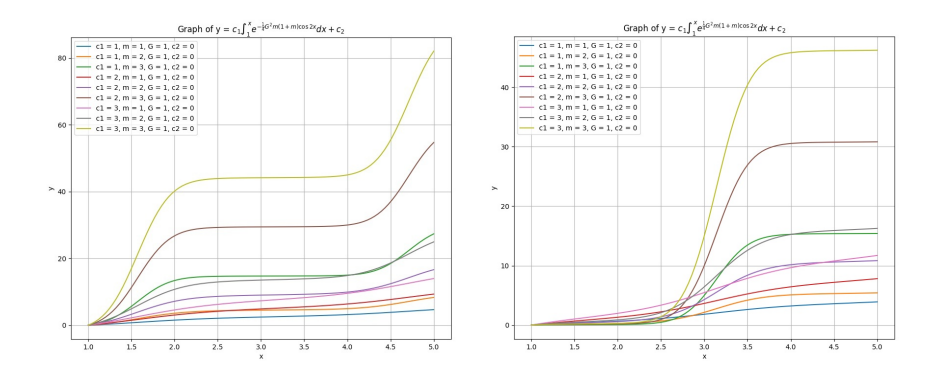


Figure 1: Variation of  $y = c_1 \int_1^x e^{\mp \frac{1}{4}G^2 m(1+m)\cos 2x} dx$  for various values of  $c_1$  and m

always positive, all curves increase monotonically, though their steepness and overall height vary. Increasing  $c_1$  scales the graph vertically, producing taller curves, while the parameter m influences the growth rate: smaller mresults in a smoother, slower rise, whereas larger m produces sharper upward bends beyond  $x \approx 3$ , leading to much faster growth (as evident in the yellow and brown curves). Between x = 2 and x = 4 several curves temporarily flatten due to the oscillatory cosine factor reducing the integrand, but all eventually rise again, demonstrating how the parameters control both the pace and magnitude of growth. In Figure 1, the second graph illustrates the variation of equation (11) under the same conditions. All curves increase monotonically because the integrand remains positive, though their profiles change with parameter values. A larger  $c_1$  scales the curves vertically, resulting in higher growth, while increasing m causes a sharper rise beyond  $x \approx 2.5$ , leading to steep bends and eventual saturation. The yellow and brown curves  $(c_1 = 3, m = 3 \text{ and } c_1 = 2, m = 3)$  exhibit the most rapid growth, approaching a plateau quickly, whereas smaller m values produce smoother, more gradual increases. Overall, the figure highlights that  $c_1$  primarily determines the amplitude, while m governs the steepness and saturation behavior of the function.

**Example 3** Cylinder with X = rx. Consider the circular cylinder  $S: Y^2 + Z^2 = r^2$ , X = rx. In parametric form, this can be expressed as

$$S: X = rx$$
,  $Y = r \sin y$ ,  $Z = r \cos y$ .

From this parametrization, we derive the following basis vectors,  $B_1$ ,  $B_2$ , and the normal vector N:

$$B_1 = (r, 0, 0), \quad B_2 = (0, r\cos y, -r\sin y), \quad N = (0, \sin y, \cos y).$$

The corresponding metric coefficients  $a_{ij}$  and the connection coefficients  $b^i$  and  $b_i$  are

$$(a_{11}, a_{12}, a_{22}) = (r^2, 0, r^2), \quad (b^1, b^2, b^0) = \left(0, \frac{-G}{r}\sin y, G\cos y\right),$$
  
 $(b_1, b_2) = (0, -Gr\sin y).$ 

Additionally, we have,  $a_x = a_y = 0$ . Then

$$\beta_{:0} = -Gr\cos yy'^2$$
 and  $\gamma = Gr\sin y$ .

Consequently, we obtain the induced metric and  $\beta$ -term:

$$\alpha^2 = r^2 (dx^2 + dy^2), \quad \beta = -Gr \sin y \, dy.$$

Therefore, equation (9) yields the approximate differential equation for the geodesic of a Matsumoto-type  $(\alpha, \beta)$ -metric (1) under the conditions of this example as

$$y'' + \frac{m(m+1)}{2}G^2(\sin 2y) \ y'^2 = 0.$$

This is a non-linear second-order differential equation for which the solution is an implicit function given by

$$x = \frac{1}{c_1} \int e^{-\frac{m(m+1)G^2}{4}\cos 2y} dy + c_2.$$
 (12)

**Example 4** Cylinder with Y = rx. We consider the circular cylinder defined by  $S: X^2 + Z^2 = r^2$  and Y = rx. In parametric form, this cylinder can be represented as

$$S: X = r \cos y, \quad Y = rx, \quad Z = r \sin y.$$

From this parametrization, we derive the following basis vectors,  $B_1$ ,  $B_2$ , and the normal vector N:

$$B_1 = (0, r, 0), \quad B_2 = (-r\sin y, 0, r\cos y), \quad N = (\cos y, 0, \sin y),$$

while the corresponding metric coefficients  $a_{ij}$  and the connection coefficients  $b^i$  and  $b_i$  are

$$(a_{11}, a_{12}, a_{22}) = (r^2, 0, r^2), \quad (b^1, b^2, b^0) = \left(0, \frac{G}{r}\cos y, G\sin y\right),$$
  
 $(b_1, b_2) = (0, Gr\cos y).$ 

Then

$$\beta_{0} = -Gr\sin yy'^2$$
 and  $\gamma = -Gr\cos y$ .

Consequently, we have the induced metric and  $\beta$ -term:

$$\alpha^2 = r^2 (dx^2 + dy^2), \qquad \beta = Gr \cos y dy.$$

Therefore, equation (9) provides the approximate differential equation for the geodesic of a Matsumoto-type  $(\alpha, \beta)$ -metric (1) under the conditions of this example:

$$y'' - \frac{m(m+1)}{2}G^2(\sin 2y) \ y'^2 = 0,$$

which has a solution

$$x = \frac{1}{c_1} \int e^{\frac{m(m+1)G^2}{4}\cos 2y} dy + c_2.$$
 (13)

**Proposition 2** The differential equations for geodesics of the Matsumoto-type metric in a two-dimensional Finsler manifold, as examined in Examples 3 and 4 for a circular cylinder, are expressed as follows:

$$y'' \pm \frac{m(m+1)}{2}G^2(\sin 2y) \ y'^2 = 0,$$

and their solutions, respectively, are expressed as

$$x = \frac{1}{c_1} \int e^{\mp \frac{m(m+1)G^2}{4} \cos 2y} dy + c_2.$$

Since the solution (12) is expressed as an implicit function, Python was employed to numerically analyze its behavior for G = 1,  $c_2 = 0$ , and varying values of  $c_1$  and m (1, 2, and 3). The resulting curves, illustrated in the first graph of Figure 2, depict the dependence of x on y for the specified parameter sets. Increasing m enhances the curvature and oscillatory nature of the curves, while variations in  $c_1$  modify the horizontal scaling, causing the profiles to stretch or compress accordingly. The parameter  $c_2$  simply translates the curves along the x-axis without affecting their shape. Overall, the figure demonstrates how changes in  $c_1$  and m influence the nonlinear mapping between x and y, producing families of smooth, S-shaped curves with distinct widths and slopes. In comparison, the second graph of Figure 2 presents the variations of functions (13) for the same parameter values. Each colored curve represents a unique parameter combination, where m primarily controls the steepness and curvature—larger m values yield more pronounced S-shaped behavior while  $c_1$  determines the horizontal scaling, compressing or expanding the curves with increasing or decreasing magnitude.

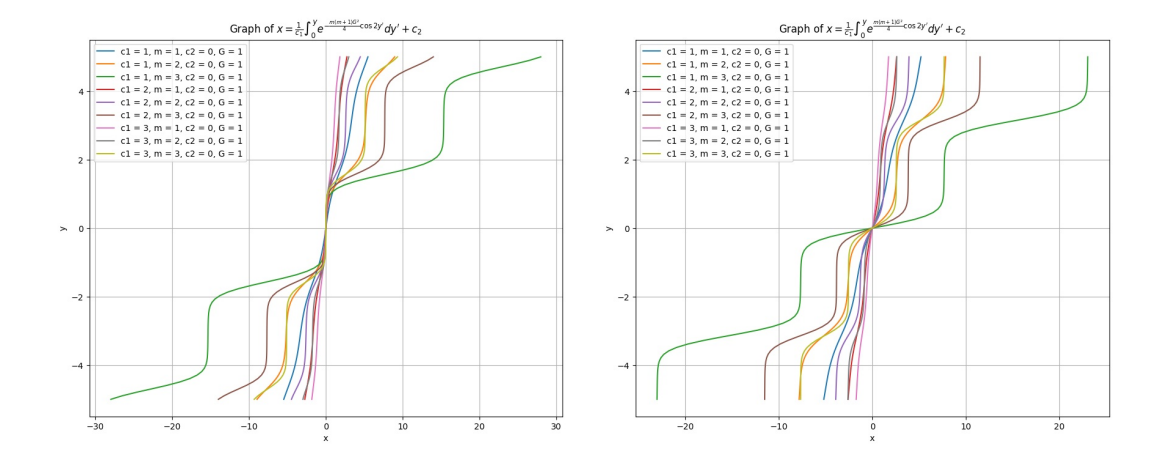


Figure 2: Variation of  $x = \frac{1}{c_1} \int e^{\mp \frac{m(m+1)G^2}{4} \cos 2y} dy$  for various values of  $c_1$  and m

**Example 5** Cylinder with Z = ry. Consider the circular cylinder defined by  $S: X^2 + Y^2 = r^2$  and Z = ry. The parametric form of this cylinder is given by

$$S: X = r \cos x, \quad Y = r \sin x, \quad Z = ry.$$

From this parametrization, we derive the following basis vectors,  $B_1$ ,  $B_2$ , and the normal vector N:

$$B_1 = (-r\sin x, r\cos x, 0), \quad B_2 = (0, 0, r), \quad N = (\cos x, \sin x, 0).$$

The corresponding metric coefficients  $a_{ij}$  and the connection coefficients  $b^i$  and  $b_i$  are

$$(a_{11}, a_{12}, a_{22}) = (r^2, 0, r^2), \quad (b^1, b^2, b^0) = \left(0, \frac{G}{r}, 0\right), \quad (b_1, b_2) = (0, Gr).$$

Then

$$\beta_{;0} = 0$$
 and  $\gamma = -Gr$ .

Consequently, we have the induced metric and  $\beta$ -term:

$$\alpha^2 = r^2 \left( dx^2 + dy^2 \right), \quad \beta = Grdy.$$

Using equation (9), we derive the approximate differential equation for the geodesic of a Matsumoto-type  $(\alpha, \beta)$ -metric (1) under these conditions as

$$y'' = 0,$$

which simplifies to the linear solution

$$y = C_1 x + C_2,$$

where  $C_1$  and  $C_2$  are constants.

**Example 6** Cylinder with Z = rx. Consider the circular cylinder defined by  $S: X^2 + Y^2 = r^2$  and Z = rx. The parametric representation of this cylinder is

$$S: X = r \cos y, \quad Y = r \sin y, \quad Z = rx.$$

From this parametrization, we derive the following basis vectors,  $B_1$ ,  $B_2$ , and the normal vector N:

$$B_1 = (0, 0, r), \quad B_2 = (-r\sin y, r\cos y, 0), \quad N = (-\cos y, -\sin y, 0),$$

and the corresponding metric coefficients  $a_{ij}$  and the connection coefficients  $b^i$  and  $b_i$  given by

$$(a_{11}, a_{12}, a_{22}) = (r^2, 0, r^2), \quad (b^1, b^2, b^0) = \left(\frac{G}{r}, 0, 0\right), \quad (b_1, b_2) = (Gr, 0).$$

Then

$$\beta_{;0} = 0$$
 and  $\gamma = Gry'$ .

Consequently, we obtain the induced metric and  $\beta$ -term:

$$\alpha^2 = r^2 \left( dx^2 + dy^2 \right), \quad \beta = Gr dx.$$

Using equation (9), we derive the approximate differential equation for the geodesic of a Matsumoto-type  $(\alpha, \beta)$ -metric (1) under these conditions as

$$y'' = 0$$
,

which simplifies to the linear solution

$$y = C_1 x + C_2,$$

where  $C_1$  and  $C_2$  are constant.

Thus, from Examples 5 and 6, we have

**Proposition 3** The differential equation for geodesics of the Matsumototype metric in a two-dimensional Finsler manifold, as analyzed in Examples 5 and 6 for a specific form of a circular cylinder, is expressed as follows:

$$y'' = 0,$$

and is solution is given by

$$y = c_1 x + c_2.$$

Futher, we use Python programming to obtain a numerical solution by setting  $c_2 = 0$ , as it acts as a shifting parameter. We examine various values of  $c_1 = 1, 2, 3$  and the results of these variations are represented as straight lines, which are shown in Figure 3.

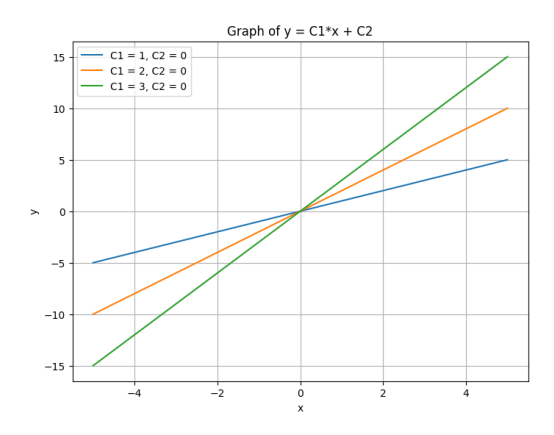


Figure 3: Variation of  $y = c_1 x + c_2$ 

## 3.2 Analysis of geodesic equations for revolution surfaces using Matsumoto-type $(\alpha, \beta)$ -metric

In this section, we analyze the geodesic equations for revolution surfaces where the axis of revolution is parallel to a constant vector field B. The surface S is given by the parametric equations

$$X = q(u)\cos y$$
,  $Y = q(u)\sin y$ ,  $Z = f(u)$ .

Using the coordinates (u, y), we derive the basis vectors  $B_1$  and  $B_2$ :

$$B_1 = (g'\cos y, g'\sin y, f'), \quad B_2 = (-g\sin y, g\cos y, 0).$$

The normal vector N is:

$$N = \frac{1}{F} \left( -f' \cos y, -f' \sin y, g' \right), \quad F = \sqrt{(f')^2 + (g')^2}.$$

The metric coefficients  $a_{ij}$  and the connection coefficients  $b^i$  and  $b_i$  are

$$(a_{11}, a_{12}, a_{22}) = (F^2, 0, g^2), \quad (b^1, b^2, b^0) = \left(\frac{Gf'}{F^2}, 0, \frac{Gg'}{F}\right),$$
  
 $(b_1, b_2) = (Gf', 0).$ 

From these coefficients, we derive

$$\alpha^{2} = F^{2} (du)^{2} + g^{2} (dy)^{2}, \quad \beta = Gf'du.$$

To convert the coordinates into an isothermal coordinate system, we take

$$x = \int \frac{F}{g} du. \tag{14}$$

With this transformation, the metric  $\alpha$  and the  $\beta$ -term become

$$\alpha^2 = g(u)^2 \left( dx^2 + dy^2 \right), \quad \beta = G \frac{f'g}{F} dx. \tag{15}$$

**Example 7** Geodesic equations on a sphere with constant curvature +1. We consider the sphere, a surface of constant curvature +1, with functions  $g(u) = r \cos u$  and  $f(u) = r \sin u$ . Here, F = r. Using the integral transformation, we obtain

$$x = \int \sec u \ du = \frac{1}{2} \log \left( \frac{1 + \sin u}{1 - \sin u} \right).$$

From  $(1 + \sin u)/(1 - \sin u) = e^{2x}$ , we find  $1/\cos u = \cosh x$ , which implies  $du = dx/\cosh x$ . Consequently, from equation (14), we derive

$$\alpha^2 = \frac{r^2}{\cosh^2 x} (dx^2 + dy^2), \quad \beta = \frac{Gr}{\cosh^2 x} dx,$$

$$(b^1, b^2, b^0) = \left(\frac{G}{r} \sec hx, 0, -G \tanh x\right), \quad (b_1, b_2) = (Gr \operatorname{sech} x, 0).$$

From here we obtain  $b_{1x} = -Gr \operatorname{sech} x \tanh x$ ,  $b_{2x} = b_{1y} = b_{2y} = 0$  and  $a = r/\cosh x$ . Thus,  $a_x = -r \operatorname{sech} x \tanh x$  and  $a_y = 0$ . Then

$$\beta_{;0} = -Gr \operatorname{sech} x \tanh x(y'^2)$$
 and  $\gamma = Gr \operatorname{sech} x(y')$ .

Therefore, (9) provides the approximate differential equation for the geodesics in the form

$$y'' = \tanh x \left\{ (1 - m(m+1)G^2)y'^3 + y' \right\}. \tag{16}$$

**Proposition 4** The differential equation for geodesics of the Matsumototype metric in a two-dimensional Finsler manifold, as examined in Example 7 for a specific form of a sphere, is given by (16).

The differential equation (16) is a nonlinear second-order differential equation. An analytical solution reveals that y = const is a trivial solution, while the general solution is quite complex. To simplify our analysis, we set G = 1, which reduces the equation to

$$y'' = \tanh x \{ (1 - m(m+1))y'^3 + y' \}.$$

The equation remains in nonlinear form; its solution is given by

$$y = \pm \int \sqrt{\frac{c_1 \cosh x}{1 - Ac_1^2 \cosh^2 x}} dx + c_2,$$

where A = 1 - m(m+1). Since the solution is analytically complex, numerical methods were employed using Python to examine its behavior for  $c_2 = 0$ 

and varying values of  $c_1 = 1, 2, 3$  and m = 1, 2, 3. The resulting variations of the curves are presented in Figure 4. The plot illustrates both the positive and negative branches of the function, represented by solid and dashed lines, respectively. Each colored pair of curves corresponds to a unique combination of parameters, as indicated in the legend. The parameter  $c_1$  primarily affects the amplitude and horizontal scaling of the curves, while m controls the rate of divergence and steepness near the origin. As  $c_1$  and m increase, the curves diverge more rapidly from the origin, indicating stronger nonlinear growth. The symmetry between the positive and negative branches confirms that the function is even in y, exhibiting mirror-image behavior with respect to the x-axis. Overall, Figure 4 highlights how variations in  $c_1$  and m govern the bifurcated nature of the function, producing symmetric pairs of curves that expand outward with distinct steepness and spread characteristics.

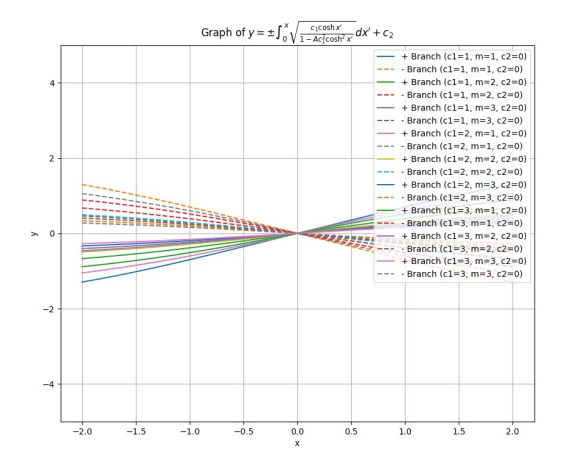


Figure 4: Variation of  $y = \pm \int \sqrt{\frac{c_1 \cosh x}{1 - Ac_1^2 \cosh^2 x}} dx + c_2$ 

**Example 8** Cylinder with constant curvature +1. We consider the cylinder, a surface of constant curvature +1, with functions g(u) = r and f(u) = u. Here, F = 1. Using the integral transformation, we obtain

$$x = \int \frac{1}{r} du, \qquad du = r dx.$$

Consequently, from equation (14), we derive

$$\begin{array}{ll} \alpha^2=r^2(dx^2+dy^2), & \beta=Grdx,\\ (b^1,b^2,b^0)=(G,0,0), & (b_1,b_2)=(G,0). \end{array}$$

From here we obtain  $b_{1x} = b_{2x} = b_{1y} = b_{2y} = 0$  and a = r. Then  $a_x = a_y = 0$  and

$$\beta_{:0} = 0, \quad \gamma = Gy'.$$

Therefore, (9) provides the approximate differential equation for the geodesics in the form

$$y'' = 0, (17)$$

which has a linear solution

$$y = C_1 x + C_2,$$

where  $C_1$  and  $C_2$  are constants.

**Proposition 5** The differential equation for geodesics of the Matsumototype metric in a two-dimensional Finsler manifold, as examined in Example 8 for a cylinder with constant curvature +1, is given by equation (17). The solution to this differential equation is the equation of straight lines.

We use Python programming to obtain a numerical solution by setting  $c_2 = 0$ , as it acts as a shifting parameter. We examine various values for  $c_1 = 1, 2, 3$  and the results of these variations are represented as straight lines, which are shown in Figure 5.

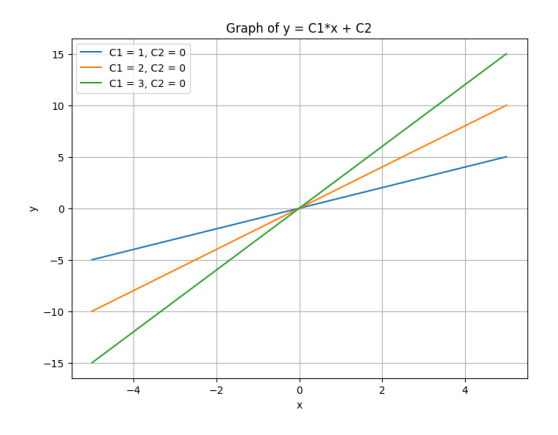


Figure 5: Variation of  $y = c_1 x + c_2$ 

**Example 9** Pseudo-sphere with constant negative curvature -1. We consider the pseudo-sphere, a surface of constant curvature -1, with the functions  $g(u) = \operatorname{sech} u$  and  $f(u) = u - \tanh u$ . The derivatives and corresponding transformations are given by

$$f' = tanh^2 u, \quad F = \tanh u$$

Using the transformation, we obtain

$$x = \int \sinh u du, \qquad du = \frac{dx}{\sinh u}$$

Substituting these into equation (14), we derive

$$\alpha^2 = \frac{1}{x^2} (dx^2 + dy^2), \quad \beta = G \frac{\sqrt{1 - x^2}}{x^2} dx,$$

$$(b^1, b^2, b^0) = \left( G, 0, -\frac{G}{x} \right), \quad (b_1, b_2) = \left( \frac{G}{x^2} (1 - x^2), 0 \right).$$

From here we obtain  $b_{1x} = -2G/x^3$ ,  $b_{2x} = b_{1y} = b_{2y} = 0$  and a = 1/x. Then  $a_x = -1/x^2$  and  $a_y = 0$ . Thus,

$$\beta_{;0} = -\frac{G}{x^3}(1+y'^2) + \frac{G}{x}(y'^2-1), \quad \gamma = \frac{G}{x^2}(1-x^2)y'.$$

Therefore, (9) yields the approximate equation of geodesics as

$$y'' = m(m+1)G^{2}\frac{(1-x^{2})}{x}y'\left[(y'^{2}-1) - \frac{(1+y'^{2})}{x^{2}}\right] + \frac{(1+y'^{2})}{x}y'.$$
 (18)

**Proposition 6** The differential equation for geodesics of the Matsumototype metric in a two-dimensional Finsler manifold, as examined in Example 9 for a pseudo-sphere with constant curvature -1, is given by (18).

The obtained equation is a highly nonlinear second-order differential equation, and its complexity makes finding an analytical solution extremely difficult, despite the existence of the trivial solution y=const. Assigning G=1 does not significantly reduce this complexity, as the equation remains challenging to solve both analytically and numerically. However, when G=0, the geometry of the manifold changes from Finslerian to Riemannian, resulting in a simplified and more tractable form of the nonlinear differential equation

$$y'' = \frac{(1+y'^2)}{r}y'. \tag{19}$$

Thus, we can state the following corollary of Proposition 6.

Corollary 1 The differential equation for geodesics of the Matsumoto-type metric in a two-dimensional Riemannian manifold, as examined in Example 9 for a pseudo-sphere with constant curvature -1, is given by (19).

The solution to the above nonlinear differential equation, obtained using Python programming, is given by

$$y = \pm \sin^{-1} c_1 x + c_2.$$

Further, we utilize Python programming to obtain a numerical solution by setting  $c_2 = 0$ , since it serves as a shifting parameter. We examine various values for  $c_1 =: 0, 0.5, 1$ . The results of these variations are given on Figure 6. It clearly illustrates that the curves for  $c_1 = 0.5$  and  $c_1 = 1$  coincide.

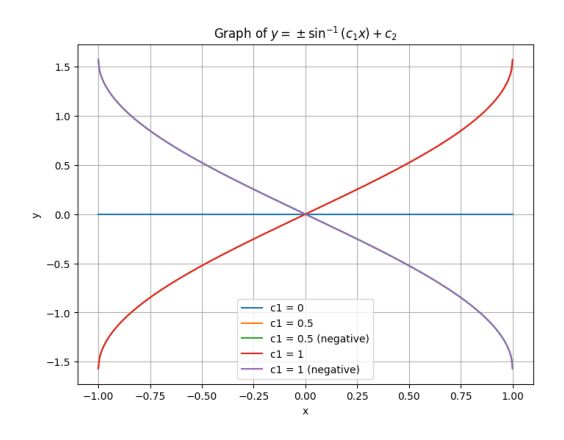


Figure 6: Variation of  $y = \pm \sin^{-1} c_1 x + c_2$ 

**Example 10** Catenoid with constant curvature -1. In this example, we consider the catenoid, a surface with constant curvature -1, with the functions  $g(u) = r \cosh u / r$  and f(u) = u. Here f' = 1 and  $F = \cosh u / r$ . Substituting integral transformation

$$x = \int \frac{1}{r} du, \qquad du = r dx,$$

into equation (14), we derive

$$\alpha^2 = r^2 \cosh^2 x (dx^2 + dy^2), \quad \beta = Gr dx,$$
  
$$(b^1, b^2, b^0) = (G \operatorname{sech}^2 x, 0, G \tanh x), \quad (b_1, b_2) = (G, 0).$$

From here we obtain  $b_{1x} = b_{2x} = b_{1y} = b_{2y} = 0$  and  $a = r \cos hx$ , and thus,  $a_x = r \sinh x$ ,  $a_y = 0$ . Then

$$\beta_{:0} = G \tanh x(y'^2 - 1), \quad \gamma = Gy'.$$

Therefore, (9) yields the following approximate equation of geodesics

$$y'' = \tanh xy' \left( \frac{m(m+1)G^2(y'^2 - 1)}{r^2 \cosh^2 x} - (y'^2 + 1) \right).$$
 (20)

**Proposition 7** The differential equation for geodesics of the Matsumototype metric in a two-dimensional Finsler manifold, as examined in Example 10 for a catenoid with constant curvature -1, is given by (20).

This is a highly nonlinear second-order differential equation, making an analytical solution extremely difficult, though the trivial solution y = const exists. Even with G = 1, the equation remains complex and challenging to solve analytically or numerically. However, setting G = 0, reduces the

system to a Riemannian manifold, simplifying the equation into a more tractable nonlinear form

$$y'' = -\tanh xy'(y'^2 + 1). \tag{21}$$

Thus, we can state the following corollary of Proposition 7.

Corollary 2 The differential equation for geodesics of the Matsumoto-type metric in a two-dimensional Riemannian manifold, as examined in Example 7 for a catenoid with constant curvature -1, is given by (21).

The solution to the above nonlinear differential equation, obtained using Python programming, is given by

$$y = \pm \int \frac{A}{\sqrt{\cosh^2 x - A^2}} dx + B.$$

Therefore, type of solution depends on the value of A. There are three types of solutions:

1. If 
$$A > 1$$
, then  $y = \pm \sinh^{-1} \frac{\sinh x}{\sqrt{A^2 - 1}} + B$ .

2. If 
$$A < 1$$
, then  $y = \pm \tan^{-1} \frac{\tanh x}{\sqrt{1 - A^2}} + B$ .

3. If 
$$A = 1$$
, then  $y = \pm \ln|\sinh x| + B$ .

Since in all the solutions, B only acts as a shifting parameter, it is set to the origin while varying A, as shown in Figures 7 and 8. In Figure 7, as A increases, the curves flatten, showing reduced steepness. The positive and negative branches are symmetric about the x-axis, indicating even functional behavior with A controlling curvature and vertical spread. Figure 8 shows both branches of  $y = \pm \ln|\sinh x|$ ; they are symmetric about the x-axis, with a singularity at x = 0 and grow nearly linearly for large |x| reflecting the logarithmic nature of  $\sinh x$ .

**Example 11** Infinite cone with constant curvature  $\theta$ . Consider the infinite cone, which has a constant curvature of zero. The parametric equations for this surface are given by g(u) = ru and f(u) = ru. To find the geodesic equations, we start with the derivatives and the corresponding transformations

$$f' = r$$
,  $F = \sqrt{2}r$ .

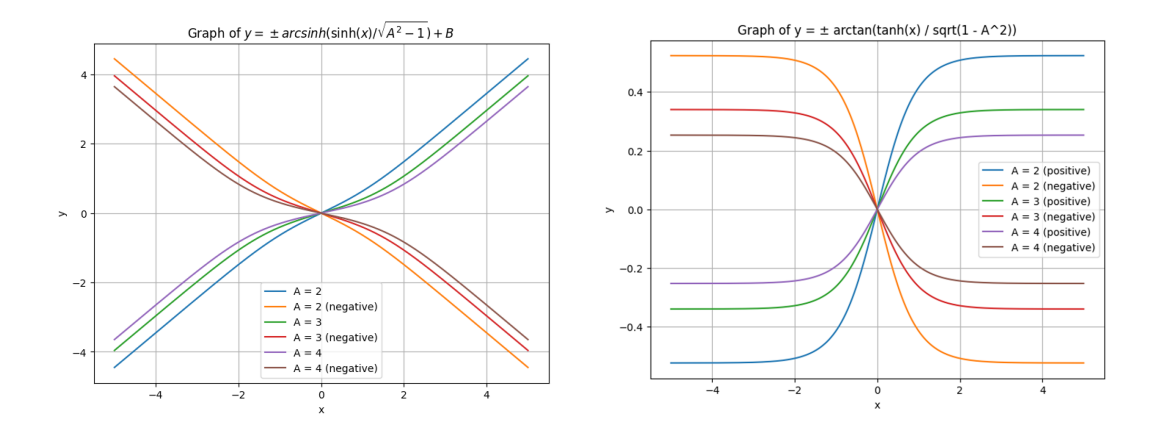


Figure 7: Variation of  $y = \pm \sinh^{-1} \frac{\sinh x}{\sqrt{A^2 - 1}} + B$  and  $y = \pm \tan^{-1} \frac{\tanh x}{\sqrt{1 - A^2}} + B$ 

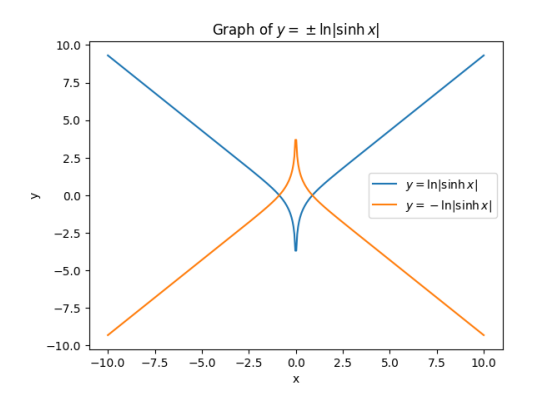


Figure 8: Variation of  $y = \pm \ln|\sinh x| + B$ 

Using equation (14), we derive the transformation  $x = \sqrt{2} \log u$ . From this, we get the relationship  $u = e^{\frac{x}{\sqrt{2}}}$ , which implies

$$du = \frac{e^{\frac{x}{\sqrt{2}}}}{\sqrt{2}}dx.$$

Using equation (15), we obtain the following expressions for  $\alpha^2$  and  $\beta$ :

$$\alpha^2 = r^2 e^{\sqrt{2}x} (dx^2 + dy^2), \quad \beta = \frac{Gr}{\sqrt{2}} e^{\frac{x}{\sqrt{2}}} dx.$$

The connection coefficients are given by

$$(b^1, b^2, b^0) = \left(\frac{G}{2r}, 0, \frac{G}{\sqrt{2}}\right), \quad (b_1, b_2) = (Gr, 0).$$

From here we determine  $b_{1x} = b_{2x} = b_{1y} = b_{2y} = 0$ ,  $a = re^{\frac{x}{\sqrt{2}}}$ , and thus,  $a_x = \frac{r}{\sqrt{2}}e^{\frac{x}{\sqrt{2}}}$  and  $a_y = 0$ . Then

$$\beta_{;0} = \frac{Gr}{\sqrt{2}}(y'^2 - 1), \quad \gamma = Gry'.$$

These expressions allow us to derive the approximate differential equation for the geodesics:

$$y'' = \frac{m(m+1)}{\sqrt{2}}G^2y'\left(y'^2 - 1\right)e^{-\sqrt{2}x} - \frac{y'}{\sqrt{2}}\left(1 + y'^2\right). \tag{22}$$

**Proposition 8** The differential equation for geodesics of the Matsumototype metric in a two-dimensional Finsler manifold, as examined in Example 11 for an infinite cone with constant curvature of zero, is given by (22).

The differential equation (22) is a second-order nonlinear equation characterized by highly complex terms, making an analytical solution extremely difficult if not impossible to obtain, despite the existence of the trivial solution y = const. To simplify the analysis, one might consider setting G = 1; however, this does not significantly ease the difficulty, as the equation remains analytically and numerically intractable. Alternatively, setting G = 0, we transform the manifold from Finslerian to Riemannian geometry. Under this condition, the equation reduces to a more manageable nonlinear form

$$y'' = -\frac{y'}{\sqrt{2}} \left( 1 + y'^2 \right). \tag{23}$$

Thus, we can state the following corollary of Proposition 8.

Corollary 3 The differential equation for geodesics of the Matsumoto-type metric in a two-dimensional Riemannian manifold, as examined in Example 11 for for an infinite cone with constant curvature of zero, is given by (23).

The solution to nonlinear differential equation (23), obtained using Python programming, is given by

$$y = \pm A \int \frac{e^{\frac{-x}{\sqrt{2}}}}{\sqrt{1 - A^2 e^{-x\sqrt{2}}}} + B.$$

Further, we use Python programming to obtain a numerical solution by setting B=0 as it acts as a shifting parameter. From the equation above, it is clear that if we set A=0, the curve will align with the y-axis. If we consider values of A greater than 1, the denominator will turn into a complex function, complicating the equation further. Therefore, we examine various values of A=0.5, 0.7, 0.9, and the results of these variations are presented in Figure 9.

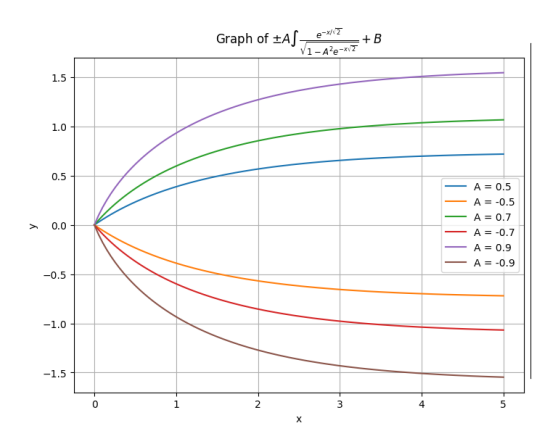


Figure 9: Variation of  $y = \pm A \int \frac{e^{\frac{-x}{\sqrt{2}}}}{\sqrt{1 - A^2 e^{-x\sqrt{2}}}} + B$ 

#### 4 Conclusion

This paper offers a thorough derivation of geodesic equations in a two-dimensional Finsler space equipped with Matsumoto-type metric, as presented in Theorem 1. It further investigates the geometric applications of these equations on various surfaces, including cylinders, spheres, pseudo-spheres, and catenoids, and provides solutions to the nonlinear differential equations of the geodesic detailed in Propositions 2–8. In cases where the analysis becomes complex and cannot be solved analytically in Finslerian space, results are derived in Riemannian space, as outlined in Corollaries 1, 2, and 3. Moreover, we employ Python programming to visualize variations through graphs, which analyze the geometric properties of geodesics. The findings significantly enhance our understanding of geodesic behavior in Finsler geometry and illuminate curvature and geometric structures in various contexts.

### References

- P.L. Antonelli, R.S. Ingarden and M.Matsumoto, The Theory of Sprays and Finsler Spaces with Applications in Physics and Biology. Kluwer Acad. Publ., Dordrecht, 1993. https://doi.org/10.1007/978-94-015-8194-3
- [2] V.K. Chaubey, A. Mishra and U.P. Singh, Equation geodesic in a two-dimensional Finsler space with special  $(\alpha, \beta)$ -metric. Bull. Transilv. Univ. Bras. III Math. Inform. Phys., **7** (56) (2014), no. 1, pp. 1–12.

- [3] V.K. Chaubey, B.N. Prasad and D.D. Tripathi, Equations of geodesic for a  $(\alpha, \beta)$ -metric in a two-dimensional Finsler space. J. Math. Comput. Sci., **3** (2013), no. 3, pp. 863–872.
- [4] I.Y. Lee and H.S. Park, Finsler spaces with infinite series  $(\alpha, \beta)$ -metric. J. Korean Math. Soc., **41** (2004), no. 3, pp 567–589. https://doi.org/10.4134/JKMS.2004.41.3.567
- [5] M. Matsumoto, Theory of Finsler spaces with  $(\alpha, \beta)$ -metric. Rep. Math. Phys., **31** (1992), no. 1, pp. 43–83. https://doi.org/10.1016/0034-4877(92)90005-L
- [6] M. Matsumoto, Foundations of Finsler Geometry and Special Finsler Spaces, Kaiseisha Press, Otsu, Japan, 1986.
- [7] M. Matsumoto, A slope of a mountain is a Finsler surface with respect to time measure. J. Math. Kyoto Univ., **29** (1989), no. 1, pp. 17–25. https://doi.org/10.1215/kjm/1250520303
- [8] M. Matsumoto and H.S. Park, Equation of geodesics in two-dimensional Finsler spaces with  $(\alpha, \beta)$ -metric. Rev. Roum. Math. Pures Appl., **42** (1997), pp. 787–793.
- [9] M. Matsumoto and H.S. Park, Equation of geodesics in two-dimensional Finsler spaces with  $(\alpha, \beta)$ -metric-II. Tensor (N.S.), **60** (1998), pp. 89–93.
- [10] T.N. Pandey and B.K. Tripathi, Two-dimensional Finsler spaces whose geodesics constitute a family of sine curves and hypocycloid. Bull. Calcutta Math. Soc., 99 (2007), no. 6, pp. 635–646.
- [11] T.N. Pandey and B.K. Tripathi, The family of cycloid and tractrix as geodesics in a two-dimensional Finsler space. J. Int. Acad. Phys. Sci. 8 (2004), pp. 51–62.
- [12] H.S. Park and I. Lee, Equations of geodesics in two-dimensional Finsler space with a generalized Kropina metric. Bull. Korean Math. Soc., **37** (2000), no. 2, pp. 337–346.
- [13] B.K. Tripathi and S. Khan, On weakly Berwald space with a special cubic  $(\alpha, \beta)$ -metric. Surv. Math. Appl., **18** (2023), pp. 1–11.
- [14] B.K. Tripathi, S. Khan and V.K. Chaubey, On projectively flat Finsler space with a cubic  $(\alpha, \beta)$ -metric. Filomat, **37** (2023), no. 26, pp. 8975–8982. https://doi.org/10.2298/fil2326975t

[15] G. Yang, On class of Einstein-reversible Finsler a met-80-103.Differ. Geom. Appl., 60 (2018),rics. pp. https://doi.org/10.1016/j.difgeo.2018.05.009

Brijesh Kumar Tripathi
Department of Mathematics,
L. D. College of Engineering,
Ahmedabad-380015, Gujarat, India.
brijeshkumartripathi4@gmail.com

Vinit Kumar Chaubey Department of Mathematics, North-Eastern Hill University, Shillong-793022, Meghalaya, India. vkcoct@gmail.com

Sejal Prajapati Science Mathematics Branch, Gujarat Technological University, Chandkheda-382424, Ahmedabad, India. sejalprajapati11198@gmail.com

## Please, cite to this paper as published in Armen. J. Math., V. 17, N. 12(2025), pp. 1–24

 $\rm https://doi.org/10.52737/18291163\text{--}2025.17.12\text{--}1\text{--}24$